CHAPTER V

Inclusion of an Antiplatelet Agent inside into β-Cyclodextrin for Biochemical Applications with Diverse Authentications

Abstract : We aim to develop the complex of ticlopidine hydrochloride (TCP) with β-cyclodextrin (β-CD) and to investigate its antibacterial and cytotoxic activities. The complex was characterized by various physicochemical as well as spectroscopic techniques suggesting the successful inclusion of TCP molecule into the β-CD cavity. TG analysis showed that the thermal stability of TCP was found to improve after complexation. Molecular docking study speculated the most preferred orientation of TCP molecule within the binding pocket of β-CD cavity. *In vitro* antibacterial activity test demonstrated that the TCP-β-CD complex displayed better activity than pure TCP. TCP-β-CD complex (IC_{50} = 24 μM) also exhibited significant *in vitro* cytotoxic activity than pure TCP (IC_{50} = 44 μM) towards human kidney cancer cell line (ACHN). Furthermore, the complex induces the ROS generation in ACHN cells more pronouncedly than TCP alone, suggesting the increased apoptotic activity of TCP after complexation. These results reveals that inclusion of TCP using β-CD could lead to stabilization of TCP and efficient display of its antibacterial and cytotoxic activities.

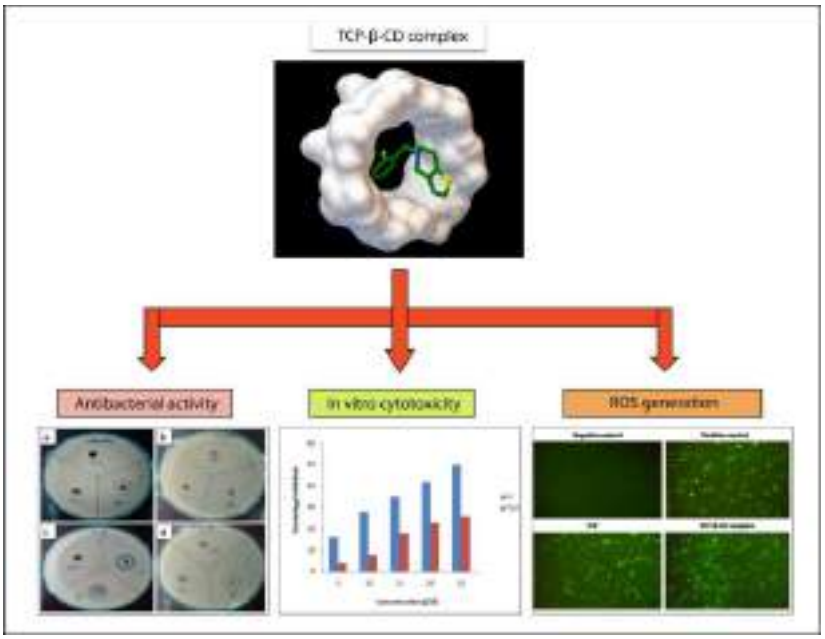

Keywords : Ticlopidine hydrochloride ; β-cyclodextrin ; Thermogravimetric analysis ; Molecular docking ; Antibacterial activity ; Cytotoxicity.

V.1. Introduction

Thienopyridine compounds act as antiplatelet agents which inhibit the formation of thrombus without markedly affecting other coagulation segments. They promote inhibition of platelet secretion reaction, inhibit platelet functions such as aggregation and adhesion, lower circulating platelet aggregates, in addition to clotting of blood in coronary artery disease, peripheral vascular disease and cerebrovascular disease.[1-3] Besides their anti-aggregating effects, thienopyridines has other pharmacological effects which include lowering circulating fibrinogen[4] as well as erythrocyte filterability[5], and stimulation of NO production[6]. Even though the actual mechanism is not understood till date, thienopyridine derivatives have demonstrated pro-apoptotic effect towards cancer cells[7] as well as anti-proliferative and anti-cancer activity against hepatocellular carcinoma[8].

Ticlopidine Hydrochloride (TCP) is one of the FDA approved drugs belonging to the family of thienopyridines which has its wide applications as antiplatelet agent. It exhibits its therapeutic effect by blocking ADP receptors irreversibly on the surface of platelets. Studies suggest that the TCP prevents clot formation and platelet aggregation inside blood vessels inhibiting development of thrombus by interacting with the $P2Y_{12}$ receptor ADP at the site of the vascular lesion through bioactivation by cytochrome P450 (CYP).[9,10] Beside antiplatelet property, TCP is also reported to have antibacterial[11] and anticancer[12] activities. However, TCP is sensitive to external conditions such as light, alkaline and acidic environment, temperature changes and oxidation,[13] which considerably demarcate its utility in terms of its anticancer and antibacterial activities. To overcome these problems one approach is encapsulation with β-cyclodextrin (β-CD). From the point of the solubilization, stabilization and delivery of the bioactive compounds, encapsulation technology is extensively used by pharmaceutical and food industries.[14] According to the previous literature, inclusion complex of β-CD improved in vitro antimicrobial activity of *Euterpe oleracea* Mart-oil[15] and in vivo anti-cancer activity of curcumin[16]. Similarly, encapsulated lycorine[17] was observed to have better in vitro cytotoxic activities. It should also be noted that β-CD was included into GRAS

(generally recognized as safe) protectants and carriers by US Food and Drug Administration.[18] β-CD is a member of cyclic oligosaccharides containing seven glucopyranose units linked via α-1,4-linkages.[19] Along with physical and chemical stability, β-CD is characterized with a relatively hydrophilic outer surface and hydrophobic central cavity. This cyclic carbohydrate, having specific cavity size (6.0–6.5 Å diameter) as well as low cost, becomes ideal for inclusion of guest molecules with molecular weights ranging from 200 to 800 g/mol.[20] After incorporation of bioactive compounds into β-CD cavity, outer microsphere of inclusion complex keeps guest molecules protected from oxygen and light.[19] To the best of our knowledge, investigation on encapsulation of TCP with β-CD and its specific antibacterial and cytotoxic activities, has not been yet studied.

Therefore, in this research, we have prepared the inclusion complex of TCP and β-CD. The physicochemical properties of prepared TCP-β-CD complex were characterized by UV-Visible spectroscopy, surface tension study, PXRD, FT-IR spectroscopy, ^{1}H NMR, TGA analysis, SEM study and mass spectroscopy. Molecular docking was performed as well to recognize the best orientation of included TCP into the cavity of β-CD. Finally, the antibacterial and cytotoxic activities of the complex were studied and compared with that of pure TCP.

V.2. Experimental section

V.2.1. Materials

Ticlopidine Hydrochloride (purity > 98%) and β-Cyclodextrin (purity 98%) were purchased from TCI Chemicals (India) and Sigma-Aldrich (India) respectively. Human kidney cancer cell lines (ACHN) were obtained from National Centre for Cell Science, Pune, India. Media component used for animal cell were purchased from Hi-media Laboratory Pvt. Ltd. MTT was purchased from Hi-media, India and DCDF dye was obtained from Sigma India Pvt. Ltd. All chemicals and media components used were of analytical grade from Sigma India Pvt. Ltd; Hi-media, India; Sisco Research Laboratories, India, TCI Chemicals, India, and E. Merck, Germany.

V.2.2. Instruments

All the UV-Visible absorption spectra were assembled at 298.15 K using the Agilent 8453 spectrophotometer, with an uncertainty of wavelength resolution of ±0.5 nm. An automated digital thermostat was used to keep the measuring temperature constant.

The surface tension was measured using a digital K9 Tensiometer (Kruss, Germany) at 298.15 K by platinum ring detachment method with measurement accuracy within ±0.1 mN m^{-1}. Temperature was maintained by auto-thermostat.

500 µL of each sample were taken into Bruker NMR tubes. Then, ^{1}H NMR spectra were acquired in D_2O at 298.15 K using Bruker Avance 300 MHz NMR spectrometer. The chemical shift values, δ, are presented in ppm. The peak of HDO at 4.70 ppm was taken as an internal standard reference.

The FT-IR spectra were recorded by KBr disk technique using Perkin-Elmer spectrometer with a 2 cm^{-1} spectral resolution at room temperature and 45% humidity. The disks were prepared by taking sample and KBr in the ratio of 1:100. The spectra were collected in the wavenumber region of 4000−400 cm^{-1}.

ESI-MS spectra were acquired on a high-resolution Q-TOF mass spectrometer with a positive-mode electrospray ionization taking the methanol solution of the solid inclusion complexes.

The samples were subject to Thermogravimetric analysis (TGA) using TA Instrument Q-50 TGA in the temperature range of 30-600 °C with the heating rate of 10° per minute.

Powder XRD data were collected on a Bruker SMART APEX diffractometer using graphite-monochromated MoK_{α} (λ=0.71073 Å) radiation equipped with CCD area detector at 273 K with scan rate 1^{0}/min and step size 0.042.

The surface morphological structure of the samples was analysed using a JSM-6360 Scanning Electron Microscope (SEM).

V.2.3. Preparation of inclusion complex

Inclusion complex of TCP with β-CD (i.e., TCP-β-CD) was prepared by mixing TCP and β-CD in a molar ratio 1:1. Initially, TCP (30 mg, 4.0 mmol) and β-CD (113.5 mg, 4 mmol) were dissolved separately in 25 mL distilled water. These two solutions were then mixed in a beaker and kept for 30 mins under moderate stirring at room temperature. Then the mixed solution was heated upto 50^0C under continuous stirring of 450 r/min for 30 hours till the appearance of a precipitate. The obtained precipitate was filtered and stored in an oven at 60^0C for 9 hours to draw out solvent. The final solid white powder of inclusion complex was collected and kept in a dessicator for further analysis.

V.2.4. Job's method for stoichiometric determination of inclusion complex

Job plot was obtained by a very reliable Job's method (also known as the continuous variation method) using UV-Visible spectroscopy to determine the complexation stoichiometry of inclusion complex formed.[21] To perform the experiment, stock solutions with equimolar concentrations of β-CD and TCP were prepared. From these two stock solutions a series of sample solutions were prepared in such a way that the overall molar concentration, [TCP]+[β-CD], was kept fixed while the mole fraction of TCP altered within the range of 0-1 (Table 1). The values of absorption maximum were recorded at λ_{max} = 214 nm for a set of solutions at 298.15 K.

V.2.5. Surface tension measurement

Ten milliliters of 10 mM TCP solution was taken in a 100 ml beaker and surface tension was measured. Then 1 ml of β-CD was added to the TCP solution for 20 times. During each addition of β-CD, surface tension reading was collected.[21]

V.2.6. Absorption spectral titrations

The inclusion complex formation phenomenon of β-CD with guest TCP in aqueous solution was examined by means of UV–Visible spectral titration.[21] During titration, one milliliter 140 μM solution of TCP was taken in a cuvette and then a series of 1.0 ml β-CD solution was added to it, so that the concentrations of β-CD ranged from 1.0-5.0 mM and that of TCP becomes 70 μM.

V.2.7. Molecular docking study

Molecular docking was conducted to predict the most probable binding mode and binding free energy (ΔG) of TCP with β-CD using automated docking progam, AutoDock 4.2.[22] The 3D structure of TCP was downloaded as SDF file from the PubChem and converted into a PDB (protein data bank) file using OpenBabel 2.4.1 software. From the RCSB Protein Data Bank, the PDB file 3CGT was downloaded and the 3D structure of β-CD was extracted from the PDB file. The optimization of the molecular structures of TCP and β-CD was performed using Gaussian 09 software with the 6-311++G (d, p) basis set and B3LYP method. Before carrying out docking, the ligand (TCP) and receptor (β-CD) coordinate files were converted into PDBQT format using MGLTools (version 1.5.6). In our docking study, β-CD was set as a rigid receptor, and TCP molecule as the flexible ligand. To seek for favourable binding mode of TCP with β-CD, a 3D docking grid box of dimension 41 Å x 41 Å x 41 Å with grid spacing 0.375 Å was constructed. Autogrid4 parameter was employed to achieve a rigid grid box. Further to acquire best docking conformations, autodock4 with Lamarckian genetic algorithm using default values was applied. On the basis of docking score, the most favourable docked conformer with lowest binding energy was selected.

V.2.8. *In vitro* antibacterial activity assay

The antibacterial activity of TCP and TCP-β-CD complex was studied using the agar well diffusion method.[23] The bacterial cultures (Shigella sp., Salmonella sp., Bacillus amyloliquefeciens and Bacillus subtilis) were grown overnight in nutrient broth at 37°C, which were further swabbed over the surface of an agar plate. Three wells were prepared in each agar plates with the help of sterile cork-borer, and 40 microlitre 6 mM solutions of β-CD, TCP and TCP-β-CD complex were introduced into their respective wells. These solutions inside the well were allowed to diffuse for an hour. Then the plates were incubated at 37^0C for 24 hours. Following incubation, plates were observed for evaluating zone of inhibition.

V.2.9. Cell line culture

For this purpose, human kidney cancer (ACHN) cell line was obtained from Cell Repository, National Centre for Cell Sciences (NCCS), Pune, India. ACHN was cultured in Dulbecco's modified eagle medium (DMEM), supplemented with 5% FBS, 100 IU ml^{-1}

Penicillin and 100 μgml^{-1} Streptomycin, in 100 mm petri dishes and incubated in 5% CO_2 incubator at 37°C.

V.2.10. *In vitro* cell viability assay

Anticancer screening of TCP and TCP-β-CD complex was carried out against human kidney cancer cell line (ACHN) by MTT [(3-(4,5-dimethylthiazol-2-yl)-2,5-diphenyltetrazolium bromide] reduction assay.[23] For a typical in vitro anticancer screening experiment, each well of 96-well microtiter plates were inoculated with 100 μl volume of cells at a concentration of 1 × 10^5 cells ml^{-1}. After cell inoculation, the microtiter plates were incubated at 37^0C for 24 hours in 5% CO_2, 95% air and 100% relative humidity. Following incubation, the cells were treated with different concentrations of TCP and its complex. After 24 hours of treatment, 10 μl of MTT (5 mg ml^{-1}) was added to each well and incubated further for 4 hours. The MTT solution was replaced by 50 μl of isopropanol which was used to dissolve the insoluble formazan product. The extent of formazan product produced due to the reduction of MTT into formazan within the cells was calculated by measuring the absorbance at 540 nm using spectrostar nano plate reader (BMG Labtech). All experiments were repeated at least three times in triplicates.The relative percentage of cell viability was evaluated by using the formula :

$$\text{Percent inhibition (\%)} = \frac{Y-X}{Y} \times 100$$

where Y is the mean absorbance of control and X is the mean absorbance of cells treated with TCP and its complex. The stock solutions of TCP and complex were prepared using distilled water and the same solvent was kept as control.

V.2.11. Determination of ROS (Reactive Oxygen Species) generation

Intracellular ROS generation can be detected using 2,7-dichlorodihydrofluorescein diacetate (DCF-DA) as a fluorescent probe.[23] DCF-DA undergoes oxidation in presence of free oxygen radicals inside the cell to fluorescent 2,7-dichlrofluorescein (DCF), which can be visualized under fluorescent microscope. Kidney cancer cell line (ACHN) were grown over the cover slip and incubated in CO_2 incubator for 24 hours. Further these cells were treated with TCP and TCP-β-CD complex at their IC_{50} values. 1.5 mM H_2O_2 treated cells were considered as positive

control whereas the untreated cells were set as a control. Following a 24 hours incubation period, the cells were washed thrice with PBS and fresh serum medium containing DCF-DA dye was added to it. It was then subjected to an incubation period of 30 min in a CO_2 incubator. After incubation, the extra dye was washed by using PBS and coverslip was flipped upside down on slide having 2-3 drops of glycerin on it. Then the cells were observed under florescence phase contrast microscope with excitation wavelength at 480 nm and emission was photographed by using Olympus digital camera.

V.2.12. Statistical analysis

All the results were processed in OriginPro 8.5 and SPPSS and all the experimental results are mean ± SD of three parallel measurements. The data were analyzed by analysis of variance ($P < 0.05$). The graph and tables have been represented with standard deviation and perform statistical analysis.

V.3. Result and Discussion

V.3.1. Determination of stoichiometric ratio of the inclusion complex by Job's method

In order to obtain the Job plot, ΔA x R versus R was plotted (where ΔA is the changes in the absorbance of TCP without and with the presence of β-CD, and R = [TCP]/([TCP] + [β-CD])). The maximal peak value of R on the plot provides the complexation stoichiometry. From Figure 1(a), the observed maximum value of ΔA x R at R = 0.5 confirms the complexation stoichiometry of 1:1 for the inclusion complex of TCP and β-CD.

V.3.2. Surface tension studies

Surface tension (γ) evaluation provides noteworthy evidence with regard to the formation and stoichiometry of the inclusion complex. [21] No any significant change in γ was observed when β-CD was dissolved in aqueous medium in an appreciable range of concentration. However, TCP solution was found to possess low γ value compared to that of pure aqueous solvent indicating that TCP is surface active molecule consisting of a hydrophobic portion and also a charged end. In this study, the γ of TCP solution was determined at 298.15 K with increasing β-CD concentration (Table 2 and Figure 1(b)). A regular increasing trend of γ was observed with increase in the concentration of β-CD,

which may be possibly due to the encapsulation of TCP molecules from the solution surface into the hydrophobic nano cavity of β-CD forming inclusion complex. A noticeable break point was found to appear in the plot indicating not only the formation of inclusion complex but also defines 1:1 stoichiometric ratio of the formed complex (Figure 1(b)). The γ value and the corresponding TCP and β-CD concentrations at the break point (point of intersection) of the surface tension curve are listed in Table 3. The ratio of the concentrations of TCP and β-CD at the break point was found to be nearly 1:1 suggesting the emergence of 1:1 inclusion complex between TCP and β-CD.K.

V.3.3. Absorption spectral analysis

The affinity for binding of TCP with β-CD was determined by evaluating binding constant (K_a) using UV spectral studies. [21] The encapsulation of TCP molecules into the apolar β-CD cavity results in the gradual increase of TCP absorbance. The occurrence of such hyperchromic shift is attributed to the decrease in polarity of the environment of β-CD cavity encountered by the TCP molecules during formation of inclusion complex. [24] The binding constant (K_a) of TCP-β-CD complex at 298.15 K was evaluated from the changes in the absorption intensity (ΔA) of TCP (at λ_{max} = 214 nm) with the increasing β-CD concentration by means of Benesi-Hildebrand equation (Table 4). According to the Benesi-Hildebrand method, a double reciprocal plot is drawn for 1:1 complexation utilizing the following Benesi-Hildebrand equation

$$\frac{1}{\Delta A} = \frac{1}{\Delta\varepsilon[TCP]K_a}\frac{1}{[\beta-CD]} + \frac{1}{\Delta\varepsilon[TCP]} \qquad (1)$$

where Δε is the difference in molar absorption coefficient of TCP in the presence and absence of β-CD. The plot of 1/ΔA against 1/[β-CD] (Figure 2) presents a good linear correlation (R^2 =0.99554) indicating 1:1 stoichiometry of the TCP-β-CD complex. The value of binding constant (K_a) for 1:1 TCP-β-CD complex, obtained from the intercept/slope of Benesi-Hildebrand plot using equation (1) [21] was found to be 25.16 x 10^3 M^{-1}.

For the encapsulation process between β-CD and TCP, the Gibb's free energy of binding (ΔG) can be deduced from the value of binding constant K_a at 298.15 K using equation (2).

$$\Delta G = - RT \ln K_a \quad (2)$$

The value of ΔG was found to be -6.0 kcal/mol, which indicates that the encapsulation process is spontaneous.

V.3.4. ^{1}H NMR analysis

^{1}H NMR study is performed for investigating the detailed information on the inclusion mechanism of guest molecule with the CDs.[25] The complexation of a guest molecule with the CD usually results in the upfield chemical shifts of both the guest and CD protons owing to the enclosure of guest molecule by the electron clouds of CD and the anisotropic ring-current effects of the encapsulated guest molecule respectively.[25] In CD, H-5' and H-3' hydrogen atoms are positioned within the cavity in the vicinity of the narrower rim and wider rim respectively, whereas the other H-4', H-2', H-1' hydrogen atoms are located on the outside of the surface (Scheme 1). In our present work, we have explored the encapsulation of TCP with β-CD using ^{1}H NMR spectroscopy. The NMR spectra of TCP, β-CD and TCP-β-CD inclusion complex were shown in Figure 3 with their corresponding chemical shift (δ) values enlisted in Table 5. After the formation of complex, H-4', H-2' and H-1' protons of β-CD were observed to possess negligible changes in their chemical shift values with Δδ −0.01, −0.01 and −0.02 respectively. However, H-5' (Δδ = −0.09) and H-3' (Δδ = −0.12) protons exhibited relatively considerable chemical shift changes, indicating the inclusion of TCP into the cavity of β-CD (Figure 3). Since H-3' proton was found to undergo significant upfield shift than H-5' proton (Table 5), therefore, it can be suggested that the encapsulation of TCP occurs through the wider rim of β-CD cavity.

Further, when we compared the ^{1}H NMR spectrum of free TCP with TCP-β-CD complex, appreciable variation in the chemical shift values was monitored for most of the TCP protons in TCP-β-CD inclusion complex. It was observed that chlorophenyl ring, piperidine ring and methylene protons such as H-12, H-13/H-14, H-15, H-4 and H-10 were greatly upfield shifted with Δδ −0.04, −0.03, −0.05, −0.04 and −0.04 respectively (Figure 3 and Table 5). In contrast, H-2 (Δδ = −0.00) and H-3 (Δδ = −0.01) protons of thiophene ring along with H-7 proton (Δδ = −0.02) of piperidine ring showed relatively negligible or no changes in their chemical shift values, suggesting that the thiophene ring along with C-7 carbon of piperidine ring resides outside the wider rim of β-CD with

the preferential occupancy of hydrophobic cavity by the chlorophenyl ring, piperidine ring and methylene group of TCP (Figure 3 and Table 5).

V.3.5. ESI-MS studies

The stoichiometry of solid TCP-β-CD inclusion complex was figured out using electrospray ionization mass spectroscopy (ESI-MS).[26] The peaks at m/z values 1399.72 and 1421.69 were observed corresponding to the molecular ions $[TCP+ \beta\text{-CD} + H]^+$ and $[TCP + \beta\text{-CD} + Na]^+$ respectively (Figure 4). This clearly indicates the formation of TCP-β-CD inclusion complex with 1:1 stoichiometric ratio, which is in conformity with the results obtained from surface tension study and Job's method.

V.3.6. Powder XRD analysis

The XRD analysis results further provides strong evidence for ensuring the inclusion complex formation. [27] The XRD patterns of β-CD, TCP and TCP-β-CD complex were shown in Figure 5(a). β-CD showed a crystalline diffractogram with sharp peaks at 4.64^0, 9.11^0, 12.47^0, 19.52^0, 21.25^0, 22.82^0, 24.30^0, 25.64^0, 27.04^0, 31.12^0, 32.06^0, 34.80^0 and 35.90^0. The TCP also exhibited a distinctive sharp peaks at 14.50^0, 16.4^0, 17.96^0, 19.29^0, 20.15^0, 22.97^0, 25.32^0, 26.03^0, 26.89^0, 27.52^0, 32.29^0 and 34.48^0, indicating the existence of TCP in a crystalline state. However, the XRD spectrum of TCP-β-CD complex displayed a broad diffraction profile with reduced number as well as intensity of peaks and showed no reflections due to either TCP or β-CD. This suggested that the moiety responsible for the crystalline nature of TCP got encapsulated into the cavity of β-CD which results in the change in environment of TCP and β-CD. This observation indicates the formation of solid inclusion complex. The appearance of new diffraction peaks at diffraction angles (2θ) of 11.80^0, 14.38^0, 15.44^0, 17.58^0, 18.64^0 and 23.94^0 revealed that the formed TCP-β-CD inclusion complex achieved a new solid state having amorphous structure, as indicated by the less intense broader diffraction peaks.

V.3.7. Analysis of FT-IR spectra

The analysis of prepared solid inclusion complex can be performed using a very useful FT-IR spectroscopic method. FT-IR spectral analysis highlights the molecular interaction of guest with host.[28] The formation of solid inclusion complex is confirmed by the variation in the peak intensity, position, shape, and its disappearance in the spectra.[28] The infrared spectra of β-CD, TCP and TCP-β-CD complex are depicted in

Figure 5(b), and the chemical bonds with their corresponding vibrational frequencies are presented in Table 6. The N-H stretching band of TCP at 3442 cm^{-1} and that of β-CD O-H at 3387 cm^{-1} were shifted to 3368 cm^{-1} as a broad band in the complex. In the case of TCP, chlorophenyl ring stretching at 1458, 1437 cm^{-1}, chlorophenyl C-H stretching at 3098, 3054, 3003 cm^{-1}, chlorophenyl C-H bending at 832, 758, 725 cm^{-1} (out-of-plane) & 1220 cm^{-1}(in-plane), C-S-C stretching at 2339 cm^{-1} and piperidine ring stretching at 1159 cm^{-1}, were observed. However, bands related to the chlorophenyl and piperidine rings in the spectrum of TCP were found to disappear in the TCP-β-CD complex spectrum, while that of C-S-C stretching observed in TCP was slightly shifted and appeared at 2341 cm^{-1} with much reduced intensity in TCP-β-CD complex. Such disappearance of IR peaks related to the chlorophenyl and piperidine rings, and the emergence of C-S-C stretching with reduced intensity indicates the inclusion of only the chlorophenyl and piperidine moieties (and not the thiophene ring) into the nano hydrophobic cavity of β-CD. The IR spectra of β-CD is characterized by C-H stretching band at 2925 cm^{-1}, C-H bending vibrations at 1410, 1362, 1334 cm^{-1}, C-O-C bending vibration at 1156 cm^{-1}, C-C-O stretching frequency at 1029 cm^{-1} and skeletal vibration involving α-1,4-linkage at 947 cm^{-1}. These vibrational bands of β-CD were shifted to 2922 cm^{-1} (C-H stretching), 1415, 1367, 1332 cm^{-1} (C-H bending), 1152 cm^{-1} (C-O-C bending), 1026 cm^{-1} (C-C-O stretching) and 943 cm^{-1} (skeletal vibration involving α-1,4-linkage) in the spectrum of solid inclusion complex, which may be possibly due to the incorporation of TCP into the β-CD cavity. All these observed variations of intensity and shifts in the IR spectra provides us the evidence of inclusion complex formation. These results suggest that the chlorophenyl and piperidine moieties (not the thiophene ring) are included into the hydrophobic cavity of β-CD, which are in good agreement with the ^1H NMR observations.

V.3.8. Thermal analysis

The TG analysis was performed on solid TCP-β-CD complex, pure TCP and β-CD to verify the thermal stability of TCP after its inclusion into CD cavity (Figure 6A). The TGA curve of β-CD exhibits a weight loss below 100^0C corresponding to the water loss and a major weight loss between 280^0C and 388^0C due to the decomposition of β-CD. For TCP, a significant weight loss was observed indicating the degradation of TCP in the range 126-250^0C. On the other hand, it can be observed from the TGA thermogram of

TCP-β-CD complex that the first stage weight loss below 89^{0}C is due to dehydration, the second one in the range 190-269^{0}C is attributed to the degradation of TCP, and the considerable weight loss after 269^{0}C indicates the main thermal decomposition of β-CD. It is evident from the TGA thermogram that the thermal decomposition of prepared complex was observed to occur at a higher range of temperature (190-269^{0}C) compared to pure TCP (126-250^{0}C), confirming that the inclusion complexation has enhanced the thermal stability of TCP.

V.3.9. SEM analysis

The study of SEM image was conducted to obtain a supporting evidence for the formation of inclusion complex by analyzing the surface morphology of solid samples.[29] Figure 6B shows the SEM microphotographs of β-CD, TCP, physical mixture and solid TCP-β-CD inclusion complex. Pure β-CD [Figure 6B (i)] had a parallelogram-like crystal structure, while TCP [Figure 6B (ii)] appeared as irregularly shaped crystal particles. In physical mixture [Figure 6B (iii)], hybrids of parallelogram-like and irregularly shaped crystals were observed, i.e., crystalline nature of both β-CD and TCP were depicted. However, solid TCP-β-CD complex [Figure 6B (iv)] appeared as unevenly shaped amorphous aggregates. Such significant modification in the surface morphology of complex confirms the encapsulation of TCP into β-CD cavity leading to the formation of solid TCP-β-CD inclusion complex.

V.3.10. Molecular docking studies

Molecular docking has been carried out for the prediction of most feasible conformation of TCP-β-CD inclusion complex with lowest binding energy (ΔG).[22] AutoDock 4.2 was used to dock a guest molecule, TCP, into the pocket of β-CD. The program produced various possible docked models according to the energetic parameters of TCP-β-CD complex. The computationally calculated free energies of binding corresponding to the ten docked conformations were listed in Table 7. Out of these ten docked conformations, four conformations 4, 5, 8 and 9 were observed to have identical structures which is reflected from their same lowest free energy of binding, -5.62 kcal/mol. One among the four lowest energy docked models of TCP-β-CD complex is shown in Figure 7. The lowest negative binding energy value (-5.62 kcal/mol)is very close to the value (-6.0 kcal/mol) calculated from the binding constant (K_a) obtained from UV-Visible spectroscopic studies, which suggest that the binding energy based on

docking result is in accordance with that deduced from UV-Visible absorption analysis. In all these four identical conformations, chlorophenyl and piperidine moieties are almost completely included into the binding pocket of β-CD, while thiophene ring was observed to lie nearly outside the wider rim. These interactions of TCP with β-CD resulted from docking analysis are in good agreement with the FT-IR and ^{1}H NMR results.

V.3.11. *In vitro* studies of biological activity

V.3.11.1. *In vitro* cytotoxicity studies

In this study, the cytotoxic effect of TCP and TCP-β-CD complex was explored against human kidney cancer cell line (ACHN). The ACHN cells were treated with various concentrations (5 μM, 10 μM, 15 μM, 20 μM and 25 μM) of TCP and complex, and the percentage inhibition of cell growth was measured by MTT assay. Figure 8 represents the dose-dependent growth inhibition of human kidney cancer cell line (ACHN) after exposure with TCP and TCP-β-CD complex. When ACHN cells are exposed with pure TCP, the IC_{50} value was found to be 44 μM. Treating the similar cells with TCP-β-CD complex gives an IC_{50} value of 24 μM. These results suggest that the complex has higher cytotoxicity and reduces the viability of tested ACHN cells more effectively than TCP alone. Hence, complexation of TCP with β-CD was found to improve the anticancer activity of TCP towards ACHN cells. This may be probably due to the sustained release of TCP from the microsphere of β-CD, which leads to greater bioavailability thus enhancing the drug effect.[30] In addition, the anticancer activity enhancement of TCP by complexation with β-CD is also likely due to the reason that β-CD can infiltrate into the drug permeation barrier, called unstirred water layer (UWL) consisting of a large number of strong H-bond networks, better than the free form of TCP. [31]

V.3.11.2. Assessment of ROS generation in ACHN cells

The overproduction of intracellular ROS (oxidative stress) could be generated not only by abnormal metabolism, but also by various drugs therapy. Oxidative stress has been widely implicated in drug-induced cytotoxicity.[32] Therefore, we evaluated the ROS production in ACHN cancer cells treated with TCP and TCP-β-CD complex at their IC_{50} values of 44 μM and 24 μM respectively. 1.5 mM H_2O_2 treated cells were considered

as positive control whereas the untreated cells were set as a control. Since in apoptosis ROS generation is an early event, the production of ROS in ACHN cells was determined after 24 hours.[33] Figure 9(a) showed that a faintly green fluorescence was observed for control indicating the formation of ROS at basal level. On the other hand, bright green fluorescence was induced in cells treated with TCP, complex and positive control, displaying a substantial amount of ROS generation [Figure 9(a)].

ROS generation was found a bit higher for TCP treated cells compared to cells exposed with positive control [Figure 9(b)]. However, TCP-β-CD complex induces significantly higher ROS generation in ACHN cells than TCP and positive control [Figure 9(b)], which reveal that the complexation with β-CD increases the apoptotic activity of TCP. These findings demonstrates that the TCP in its complex form is more effective for oxidative mediated apoptosis than TCP alone due to ROS hyper-generation. Therefore, the induction of increased intracellular ROS (oxidative stress) production by TCP-β-CD complex could be one of the reasons for the observation of greater cytotoxicity of the complex towards ACHN cells compared to free TCP.

V.3.11.3. *In vitro* antibacterial activity studies

The treatment of cancer with chemotherapeutic agents/drugs may lead to secondary complications of weakening the immune system and in some cases causing immunodeficiency. Therefore, cancer patients are more vulnerable to develop various types of microbial infections. According to reports, microbial infections remain a significant cause of mortality among cancer patients.[34] Thus, there is an unfulfilled and unresolved need for a drug which not only has anti-cancer properties but also has antibacterial properties. The drug having such effect could lead to reduce the secondary complications and thus improve the chances of recovery and survival of cancer patients. Therefore, we performed the antibacterial test using the agar diffusion technique with four bacteria, namely, *Salmonella sp.*, *Shigella sp.*, *B. amyloliquefaciens* and *B. subtilis*, to evaluate the antibacterial activity of TCP and TCP-β-CD complex. Both TCP and TCP-β-CD complex showed noteworthy antibacterial activity against these bacteria (Figure 10). However, it can be seen from the Table 8 that the complex was found to possess relatively greater inhibitory effect than TCP alone. This indicates that the complex possessed effectively higher antibacterial activity than pure TCP, which may be possibly due to the fact that β-CD transports TCP readily to the surface of bacterial cells.[35]

Another factor for this is presumably the complexation of TCP with β-CD significantly improved the bioavailability of TCP due to the improvement of the solubility.[36]

V.4. Conclusion

We have reported the successful preparation of TCP-β-CD complex and examined the effect of inclusion on the *in vitro* bioactivity of TCP. The formulation of complex was confirmed by ^{1}H NMR, ESI-MS, FT-IR, TGA, SEM, PXRD, surface tension and UV-Visible spectroscopic studies. The Job's method, surface tension study and ESI-MS experiment confirmed 1:1 stoichiometry of the TCP-β-CD complex. Higher binding constant value (K_a = 25.16 x 10^3 M^{-1}) accounts for the higher binding affinity of TCP with β-CD and the thermodynamic spontaneity of binding process was validated by the negative Gibb's free energy change (ΔG). ^{1}H NMR, FT-IR and molecular docking studies suggested a possible stable molecular conformation for TCP-β-CD complex in which the chlorophenyl and piperidine moieties are almost completely included into the cavity of β-CD, and the thiophene ring lie nearly outside the wider rim. PXRD and SEM analysis showed that the prepared complex has amorphous nature which is unlike from its pure components. From TGA analysis we observed that encapsulation has enhanced the thermal stability of TCP. *In vitro* antibacterial test showed that the better activity was displayed by TCP after its complexation with β-CD. TCP-β-CD complex (IC_{50} = 24 μM) expressed significant cytotoxic effect than pure TCP (IC_{50} = 44 μM) towards human kidney cancer cell line (ACHN). Furthermore, the complex was found to induce the intracellular ROS generation more prominently than TCP, suggesting the enhancement in the apoptotic activity of TCP after complexation. Thus, TCP-β-CD inclusion complex can be a promising approach for designing a novel formulation of TCP in drug delivery, thereby, extending the potential clinical purpose of TCP in pharmaceutical industries and biomedical sciences.

Tables

Table 1. Data for the Job plot performed by UV-Visible spectroscopy for aqueous TCP-β-CD system at 298.15K[a]

TCP (mL)	β-CD (mL)	TCP (μM)	β-CD (μM)	[TCP]/([TCP]+[β-CD])	Absorbance (A)	ΔA	ΔA×[TCP]/([TCP]+[β-CD])
0	3	0	70	0	0	0.59898	0
0.3	2.7	7	63	0.1	0.0885	0.51048	0.05105
0.6	2.4	14	56	0.2	0.14469	0.45469	0.09094
0.9	2.1	21	49	0.3	0.22375	0.37523	0.11257
1.2	1.8	28	42	0.4	0.27627	0.32271	0.12908
1.5	1.5	35	35	0.5	0.31897	0.28001	0.14
1.8	1.2	42	28	0.6	0.37574	0.22324	0.13394
2.1	0.9	49	21	0.7	0.43502	0.16396	0.11477
2.4	0.6	56	14	0.8	0.49597	0.10301	0.08241
2.7	0.3	63	7	0.9	0.56515	0.03383	0.03045
3	0	70	0	1	0.59898	0	0

[a]Standard uncertainties in temperature u are: u(T) = ±0.01 K.

Table 2. Data for surface tension study of aqueous TCP-β-CD system at 298.15K[a]

Volume of β-CD (mL)	Total volume (mL)	Conc. of TCP (mM)	Conc. of β-CD (mM)	Surface tension (mN m^{-1})
0	10	10.000	0.000	61.6
1	11	9.091	0.909	63.2
2	12	8.333	1.667	64.1
3	13	7.692	2.308	65.5
4	14	7.143	2.857	66.2
5	15	6.667	3.333	67.0
6	16	6.250	3.750	67.9
7	17	5.882	4.118	68.3
8	18	5.556	4.444	68.9
9	19	5.263	4.737	69.3
10	20	5.000	5.000	69.6
11	21	4.762	5.238	69.8
12	22	4.545	5.455	70.0
13	23	4.348	5.652	70.1
14	24	4.167	5.833	70.2
15	25	4.000	6.000	70.2
16	26	3.846	6.154	70.3
17	27	3.704	6.296	70.3
18	28	3.571	6.429	70.4
19	29	3.448	6.552	70.4
20	30	3.333	6.667	70.5

[a]Standard uncertainties in temperature u are: u(T) = ±0.01 K.

Table 3. Values of surface tension (γ) at the break point with corresponding concentrations of β-CD and TCP at 298.15 K.

Concentration of β-CD (mM)	Concentration of TCP (mM)	γ (mN m^{-1})
4.94	5.06	69.7

Table 4. Data for the Benesi-Hildebrand double reciprocal plot performed by UV-Visible spectroscopy for aqueous TCP-β-CD system at 298.15 K[a] ; ± indicates the standard deviation

TCP (μM)	β-CD (mM)	A_o	A	1/[β-CD] (M^{-1})	1/ΔA	Intercept	Slope	K_a x10^{-3} (M^{-1})
70	1.0		0.64123	1000	23.66864			
70	2.0		0.64207	500	23.20724			
70	3.0	0.59898	0.64228	333	23.09469	22.76486	0.000904651	25.16±0.83
70	4.0		0.64248	250	22.98851			
70	5.0		0.64259	200	22.93052			

[a]Standard uncertainties in temperature u are: u(T) = ±0.01 K.

Table 5. ^{1}H NMR data of pure TCP, β-CD and TCP-β-CD complex in D_2O

H protons	ppm (D_2O)			Δδ = $\delta_{complex}$- δ_{TCP}	Δδ = $\delta_{complex}$- $\delta_{β-CD}$
	δ_{TCP}	$\delta_{β-CD}$	$\delta_{complex}$		
H-2	7.27	–	7.27	0.00	–
H-3	6.74	–	6.73	-0.01	–
H-4	4.29	–	4.25	-0.04	–
H-6	3.54	–	–	–	–
H-7	3.14	–	3.12	-0.02	–
H-10	4.54	–	4.50	-0.04	–
H-12	7.42	–	7.38	-0.04	–
H-13, H-14	7.36	–	7.33	-0.03	–
H-15	7.50	–	7.45	-0.05	–
H-1’	–	4.97	4.95	–	-0.02

H-2’	–	3.56	3.55	–	-0.01
H-3’	–	3.87	3.75	–	-0.12
H-4’	–	3.49	3.48	–	-0.01
H-5’	–	3.76	3.67	–	-0.09

Table 6. FT-IR data of pure TCP, β-CD and TCP- β-CD complex

TCP	β-CD	TCP- β-CD complex
3442 cm^{-1} : N-H stretching **1458, 1437 cm^{-1} :** chlorophenyl ring stretching **3098, 3054, 3003 cm^{-1}** :chlorophenyl C-H stretching **832, 758, 725 cm^{-1}** :chlorophenyl C-H bending (out-of-plane) **1220 cm^{-1}** :chlorophenyl C-H bending (in-plane) **1159 cm^{-1}** :piperidine ring stretching	**3387 cm^{-1} :** O-H stretching **2925 cm^{-1} :** C-H stretching **1410, 1362, 1334 cm^{-1} :** C-H bending **1156 cm^{-1} :** C-O-C bending **1029 cm^{-1} :** C-C-O stretching **947 cm^{-1} :** skeletal vibration involving α-1,4-linkage	**3368 cm^{-1} :** N-H/O-H stretching **2922 cm^{-1} :** C-H stretching **1415, 1367, 1332 cm^{-1} :** C-H bending **1152 cm^{-1} :** C-O-C bending **1026 cm^{-1} :** C-C-O stretching **943 cm^{-1} :** skeletal vibration involving α-1,4-linkage **2341 cm^{-1} :** C-S-C stretching

Table 7. Calculated binding energies of different docked conformations of TCP-β-CD inclusion complex

Run	Final Intermolecular Energy (kcal/mol)	Vander waal + H-bond + desolv Energy (kcal/mol)	Electrostatic Energy (kcal/mol)	Final Total Internal Energy (kcal/mol)	Torsional Free Energy (kcal/mol)	Unbound System's Energy (kcal/mol)	Estimated Free Energy of Binding (kcal/mol)
1	-5.91	-5.93	+0.02	-0.53	+0.6	-0.53	-5.32
2	-5.92	-5.94	+0.02	-0.55	+0.6	-0.55	-5.32
3	-5.92	-5.95	+0.02	-0.54	+0.6	-0.54	-5.33
4	-6.22	-6.29	+0.07	-0.51	+0.6	-0.51	-5.62
5	-6.21	-6.27	+0.05	-0.50	+0.6	-0.50	-5.62
6	-5.94	-5.95	+0.02	-0.54	+0.6	-0.54	-5.34
7	-5.94	-5.96	+0.02	-0.54	+0.6	-0.54	-5.34

8	-6.22	-6.29	+0.07	-0.51	+0.6	-0.51	-5.62
9	-6.22	-6.27	+0.06	-0.50	+0.6	-0.50	-5.62
10	-5.93	-5.94	+0.02	-0.55	+0.6	-0.55	-5.33

Table 8. Zone of inhibition of TCP and TCP-β-CD complex against different bacteria.± indicates the standard deviation

	Zones of Inhibition (mm)		
Bacteria	TCP	TCP-β-CD complex	β-CD
Salmonella sp.	11±0.62	16±0.85	-
Shigella sp.	10±0.18	16±0.62	-
Bacillus amyloliquefaciens	15±0.82	16±0.60	-
Bacillus subtilis	11±0.60	17±0.62	-

Figures

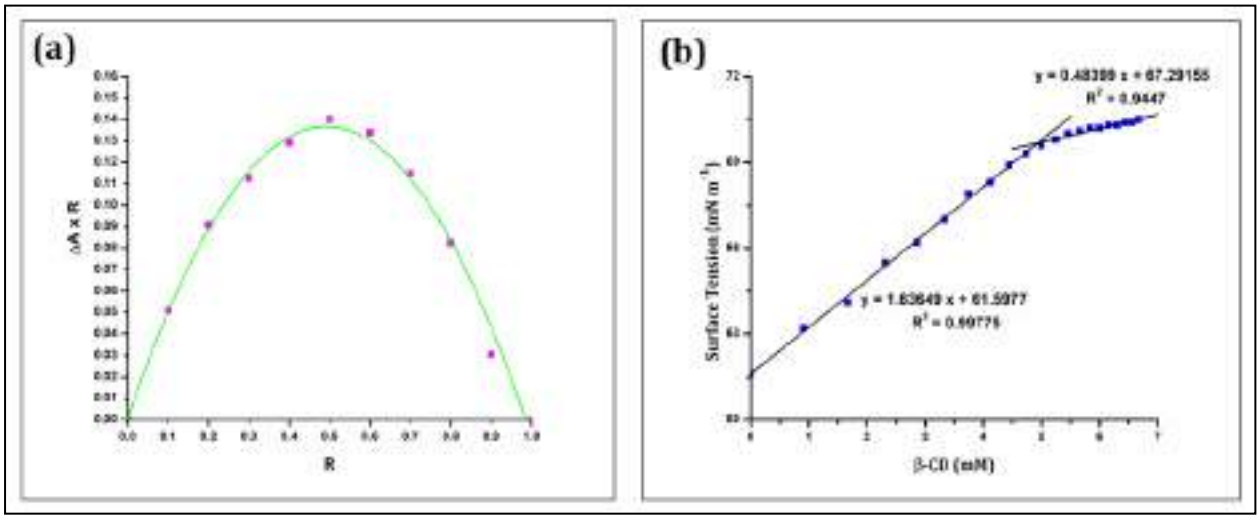

Figure 1. (a) Job plot for TCP-β-CD system at 298.15 K (λ_{max} = 214 nm) ; **(b)** Surface tension variation of aqueous TCP solution with increasing β-CD concentration at 298.15 K.

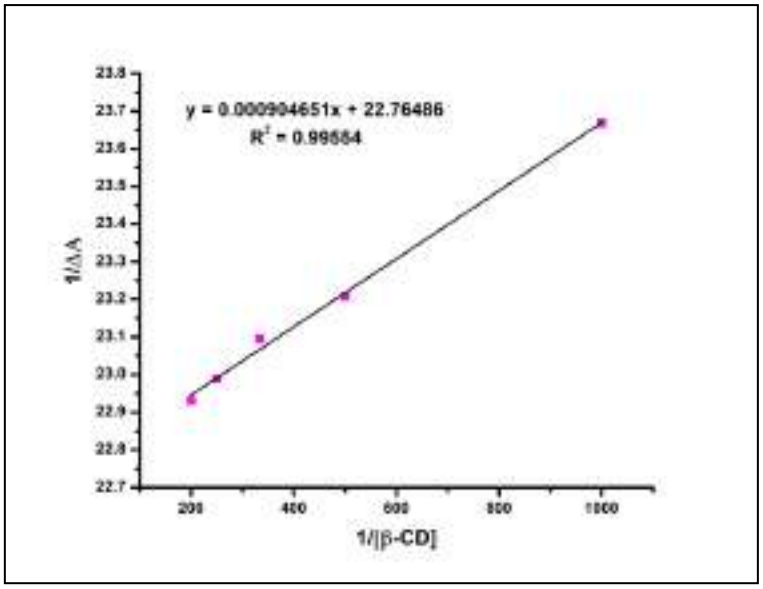

Figure 2. Benesi-Hildebrand double reciprocal plot for the effect of β-CD on the absorbance of TCP (λ_{max} = 214 nm) at 298.15 K.

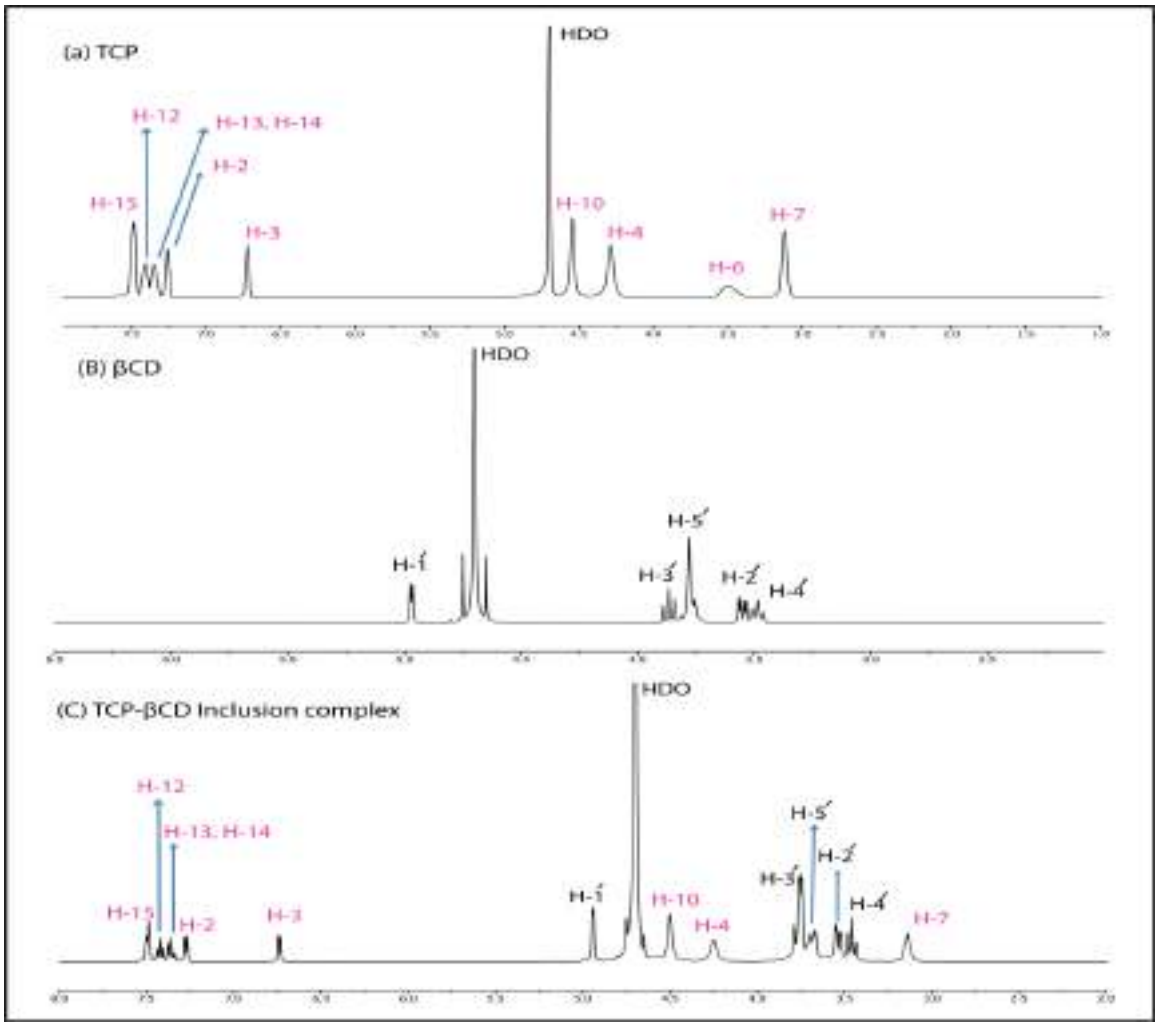

Figure 3. ^{1}H NMR spectra of TCP, β-CD and TCP-β-CD complex in D_2O at 298.15K.

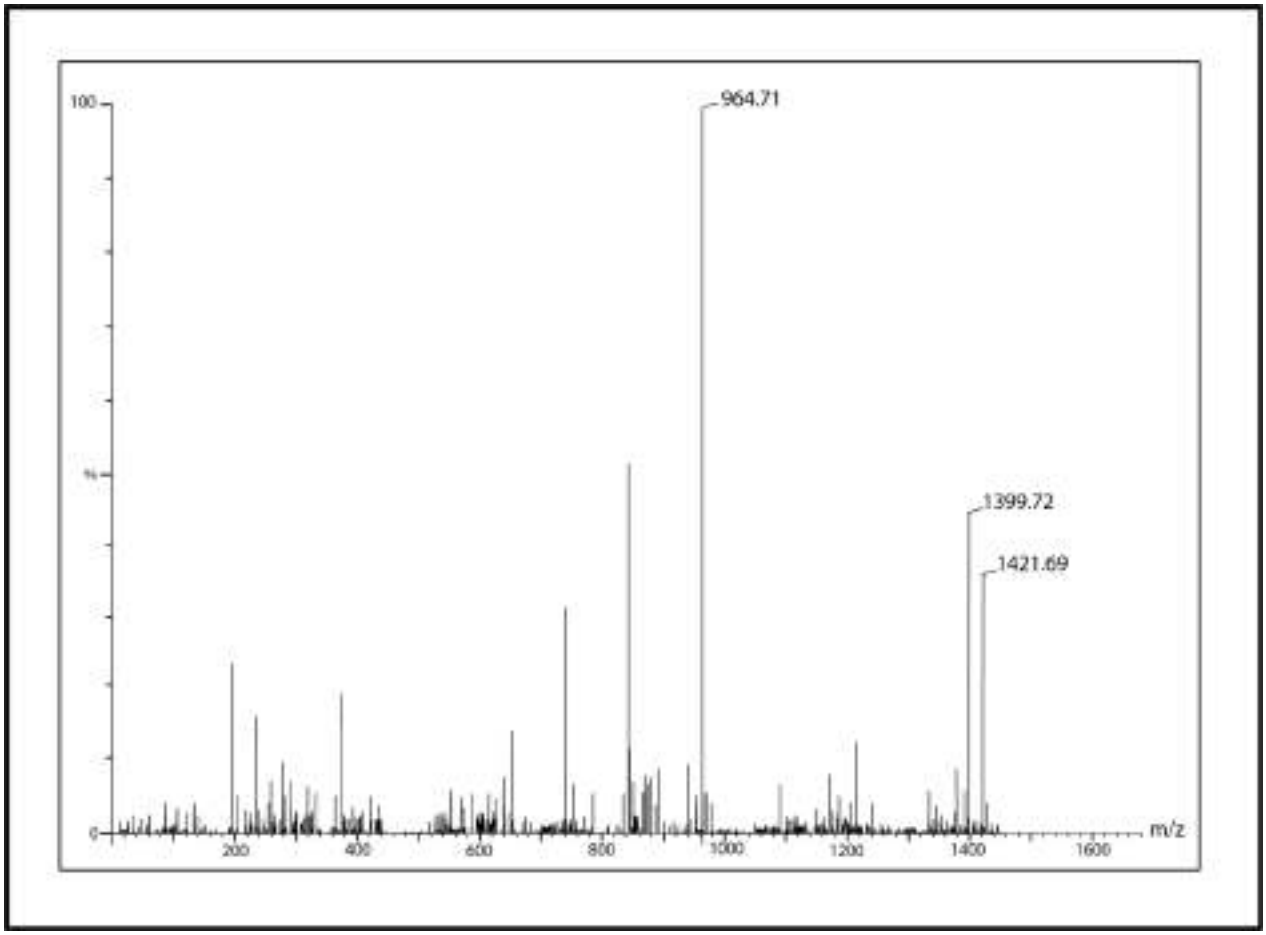

Figure 4. ESI-MS mass spectra of TCP-β-CD complex in D_2O at 298.15K.

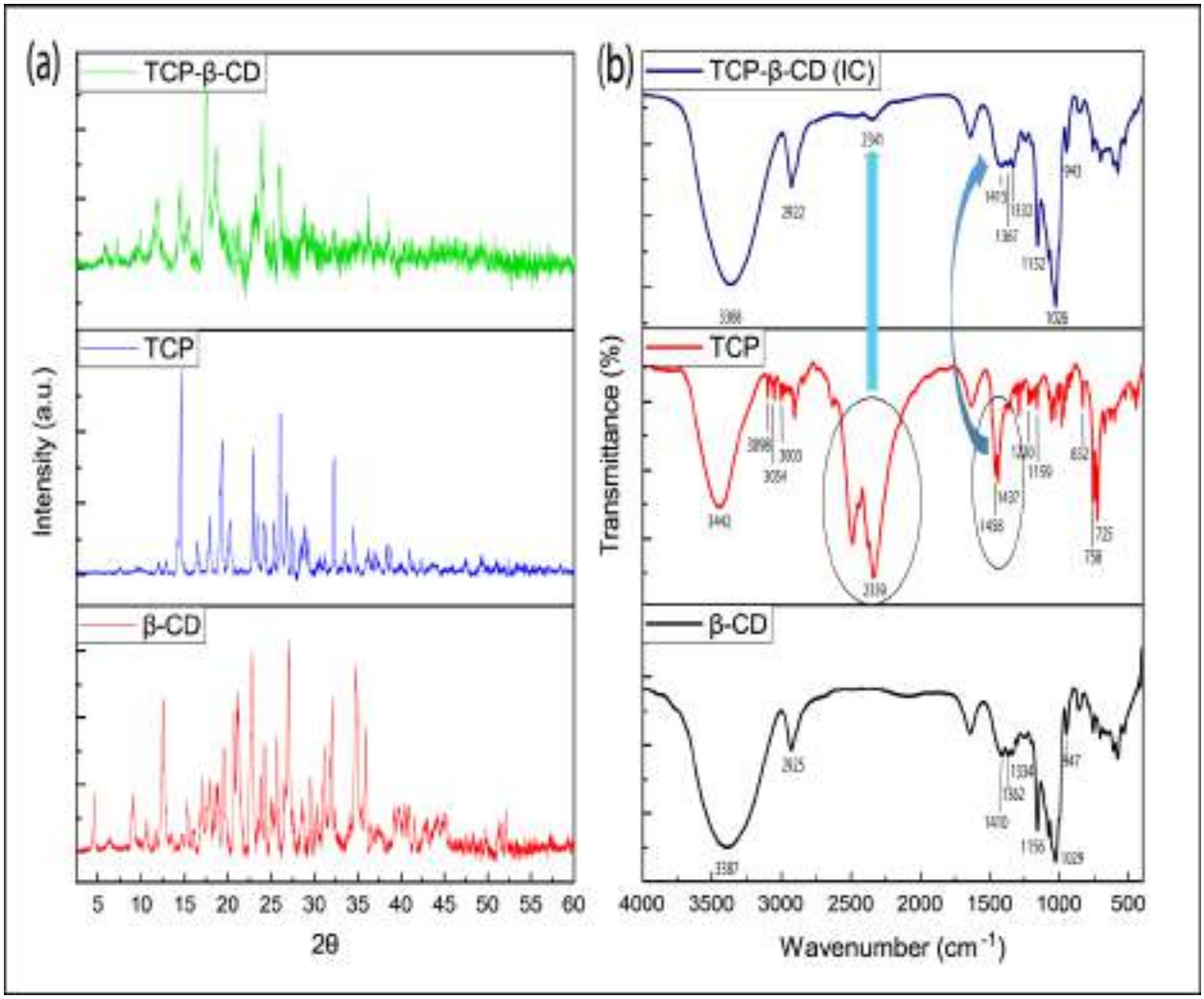

Figure 5. (a) PXRD profiles and **(b)** FT-IR spectra of β-CD, TCP and solid TCP-β-CD inclusion complex.

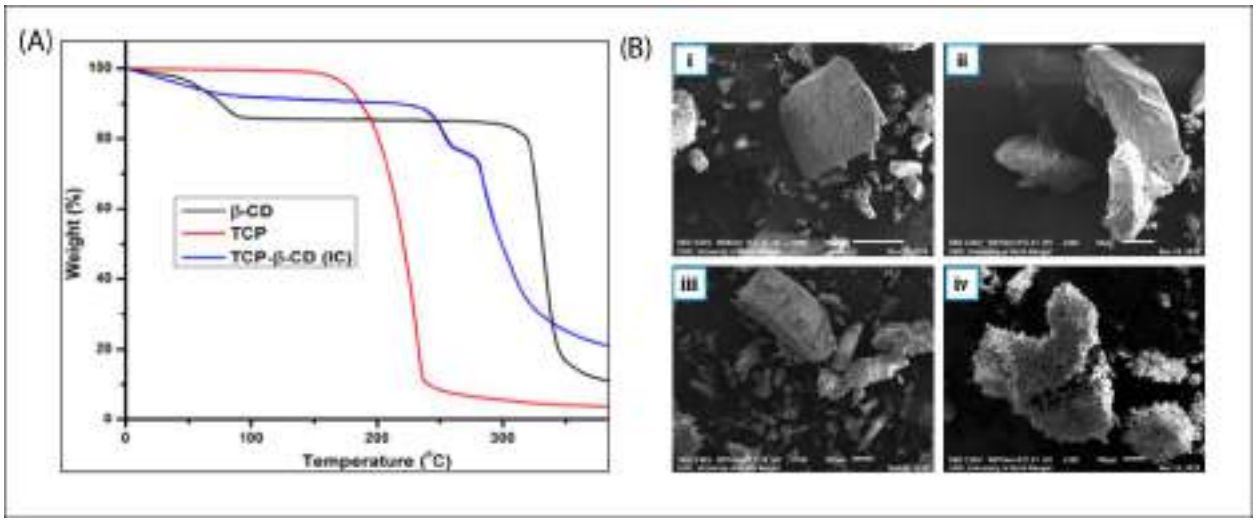

Figure 6. (A) TGA thermograms of TCP, β-CD and TCP-β-CD inclusion complex ; **(B)** Scanning electron micrographs : (i) β-CD, (ii) TCP, (iii) physical mixture of TCP and β-CD, (iv) TCP-β-CD inclusion complex.

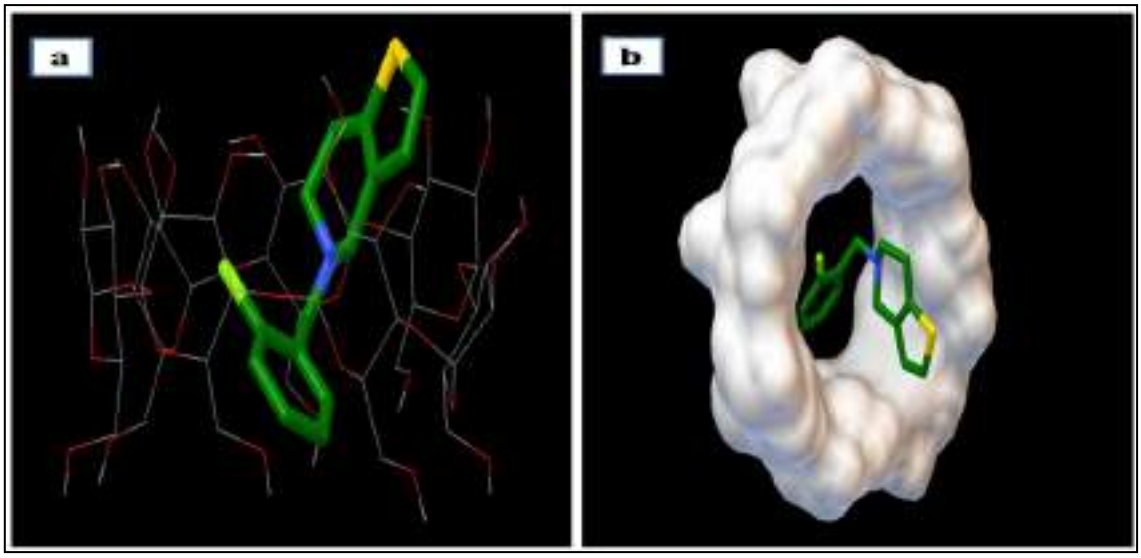

Figure 7. Docked conformation of TCP-β-CD inclusion complex, side view **(a)** and top view **(b)**.

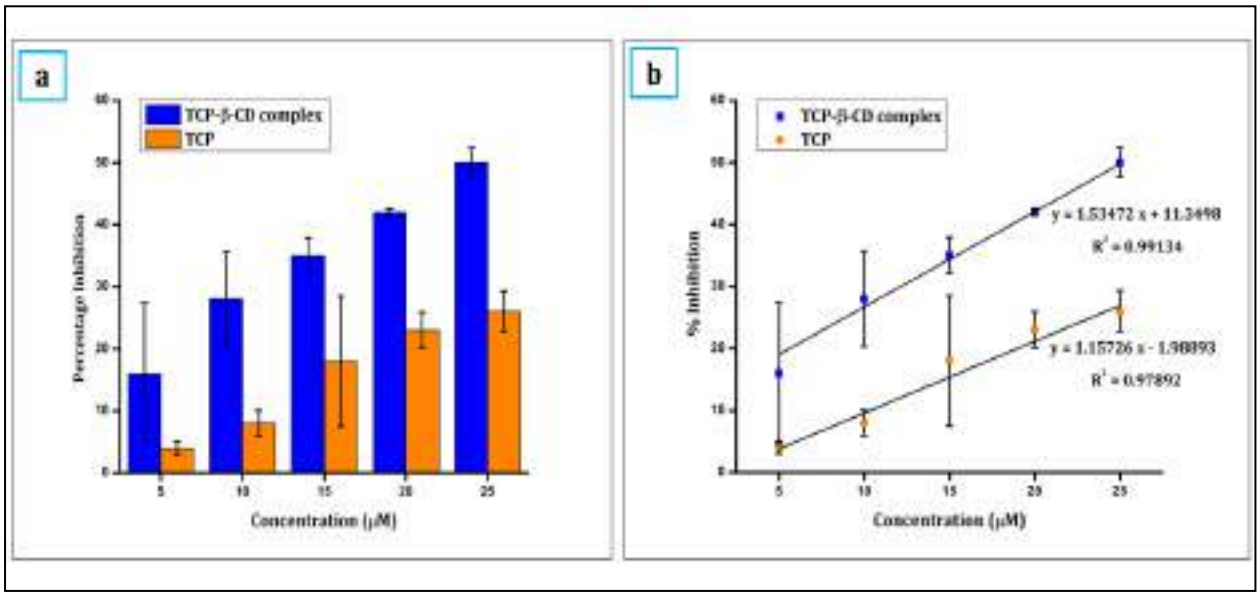

Figure 8. (a) Dose-dependent growth inhibition of human kidney cancer cell line (ACHN) after exposing with TCP and TCP-β-CD complex for 48 hours, **(b)** Linear regression analysis to calculate IC_{50} values. The obtained results are from three separate experiments presented as mean ± standard deviation.

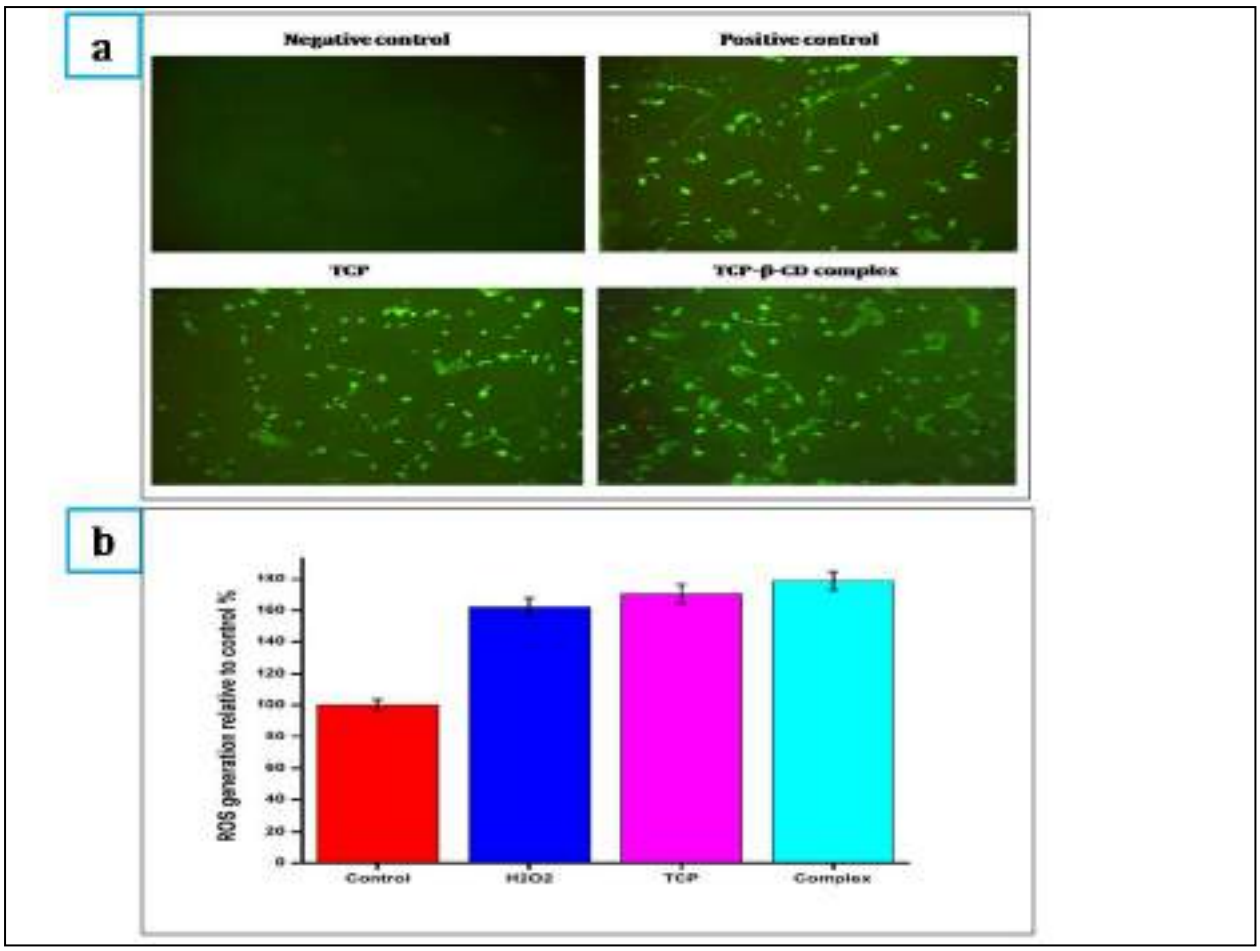

Figure 9. Evaluation of intracellular ROS generation in ACHN cells using the fluorescent probe DCF-DA. **(a)**Photomicrographs of the untreated cells (negative control) and the cells treated with TCP (IC_{50} = 44 µM), TCP-β-CD complex (IC_{50} = 24 µM) and positive control (1.5 mM H_2O_2) for 24 hours. **(b)** Percentage of ROS generation relative to control. The obtained results are presented as mean ± standard deviation.

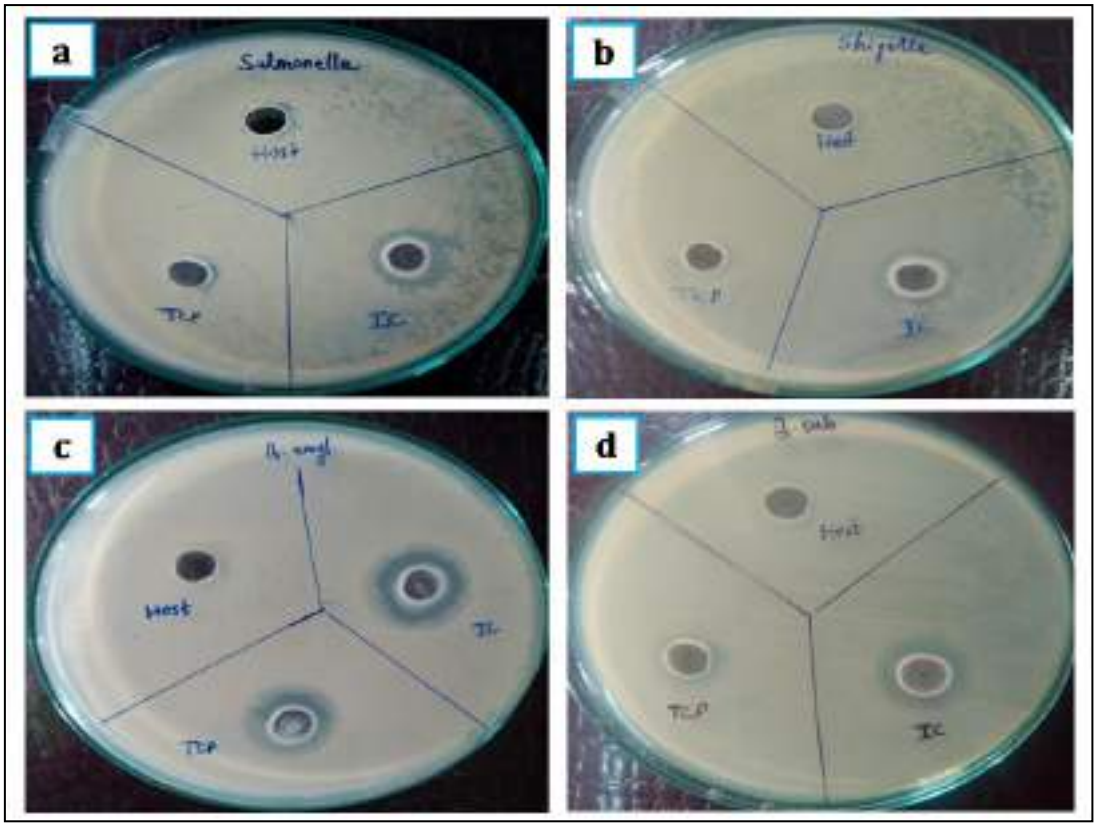

Figure 10. Antibacterial effect of TCP and TCP-β-CD inclusion complex against different microbial organisms, i.e., two Gram-negative bacteria **(a)** Salmonella sp. **(b)** Shigella sp., and two Gram-positive bacteria **(c)** B. amyloliquefaciens **(d)** B. subtilis.

Schemes

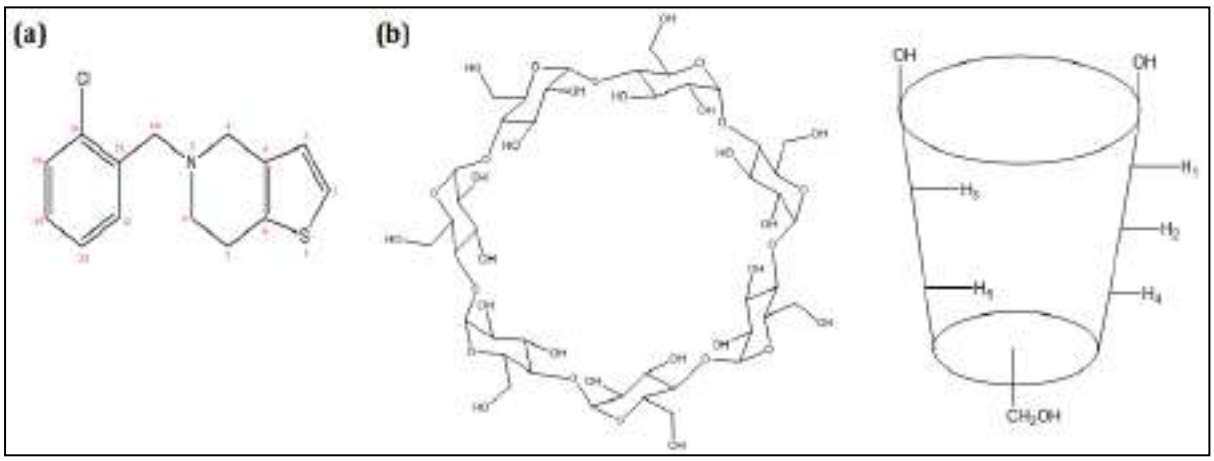

Scheme 1. Molecular Structures of **(a)** TCP and **(b)** β-CD.